

EDWIN ROEDDER

Application of studies of fluid inclusions in salt samples to the problems of nuclear waste storage

ABSTRACT: The fluids present as fluid inclusions in salt samples from various bedded and domal salt deposits provide a surprising amount of information on the saline environment throughout the geological history of the deposit. Such information is valuable in considerations of the possible future history of these deposits, should they be used for long-term nuclear waste storage sites. In addition, however, the fluid inclusions (and other varieties of water) present in the salt are of considerable importance to the safe design and operation of such sites, and most analyses of salt for water are erroneously low. Fluid inclusions will generally migrate up the thermal gradients, toward the waste canisters, and contain highly corrosive fluids.

INTRODUCTION

Salt deposits, either bedded or domal, were first considered during the 1950's as possible sites for storage of nuclear waste, in part, on the evidence that salt mines were generally very dry places*. Since then there has been a continuing interest in the amount of water that might be encountered in the use of salt deposits for repositories. Two entirely separate sources of water need to be considered, external and internal. Any subsurface cavity can become saturated with external water under the proper hydrostatic conditions. Numerous salt mines in the United States and abroad have been flooded, sometimes suddenly (*e. g.* Baar 1977, Martinez & Wilcox 1976), despite precautions.

The internal (*in situ*) water is much less obvious, although at least some water is always present in what appears visually to be comple-

* The paper bears data included from a series of publications (Roedder & Bassett 1981; Roedder & Belkin 1979a, b, 1980 a, b; Stewards & al. 1980)

tely dry rock salt. The exact nature of this *in situ* water, and particularly the amounts present, are of considerable importance to the design and performance of nuclear-waste storage facilities in salt (Stewart & al. 1980). The amount of such water that may be released through heating of the rock salt by the radioactive waste, and its probable composition, pressure, and temperature, must be taken into account in the design of the waste form, corrosion-resistant canister, over-pack, and backfill (McCarthy 1979, Northrup 1980). The water must also be considered in designing the repository itself, because water lowers the physical strength of rock salt, particularly at elevated temperatures. Thus, accurate determinations of the water contents of rock salt samples from various prospective sites are needed during the preliminary site evaluation and selection process. Many such determinations have been made by a wide variety of physical and chemical methods that do not (and cannot) give truly comparable results. Problems with the determinations themselves are such that they are neither trivial nor routine matters. In this paper I discuss the nature of the fluid inclusions present, the data that can be obtained from them, the problems that they may cause in the use of such salt deposits for nuclear waste disposal and some of the problems in the analysis of salt samples for water content.

NATURE OF THE SAMPLES

Most of the samples used in this study were test cores (≈ 10 cm diameter), bored using saturated brine as drilling fluid. In all locations, the samples were selected in part to be representative of the various lithologies visible in the cores, and in part to obtain material most likely to contain useful inclusions, based on visual inspection and past experience. From the Waste Isolation Pilot Plant (hereafter called "WIPP") site in SE New Mexico, 19 core samples were obtained from the ERDA No. 9 borehole, mostly from the two specific depth intervals being considered for repositories, but including samples from 1979 ft to 2821 ft depth. Eight samples from the Rayburn dome, Bienville Parish, Louisiana (D.O.E. — C. F. I. No. 1 core), ranging from 168 ft to 1971 ft depth, and ten from the Vacherie dome, Webster Parish, Louisiana (D.O.E. Smith No. 1 core), ranging from 561 ft to 3222 ft depth were studied. From the Palo Duro Basin, Texas, 15 sections of core were studied, from 1200 to 3350 ft depth. Other samples, from numerous other locations, were examined less intensively, including bedded salt from Hutchinson, Kansas and Goderich, Ontario, and domal or anticlinal salt from Asse, F.R.G.; Anderbeck, Halle, and the Werra district, D.D.R.; Wieliczka and Kłodawa, Poland; and from Vera Cruz, Mexico. The bulk of the work has been on the New Mexico samples, so they are discussed in more detail.

METHODS USED AND THEIR APPLICATION

PETROGRAPHIC MICROSCOPE

Standard, normal petrographic examination was used on all samples to aid in an understanding of the origin, mineralogy, and geological history of these evaporites, and to anticipate what problems the inclusions might cause during long-term storage of high-level (i.e. highly radioactive and heat-producing) wastes. But for such studies to have maximum usefulness and minimum ambiguity, special sample preparation methods are essential. Salt samples fracture very readily from rough handling and from even the mild heating that can occur during grinding and polishing, so considerable care is needed. Slow speed, continuous-rim diamond wheels, or slow-speed, fine-wire saws were used in the cutting, followed by hand grinding, using saturated brine as lubricant. Final polishing with $0.3 \mu\text{m Al}_2\text{O}_3$, is done (also by hand) or dryer and dryer paper laps. Most samples were examined as doubly polished slabs up to 1 cm thick. Since the exact nature of the grain boundaries is very important, reflected light microscopy was used extensively; this requires special care, as minor differences in polishing procedure can change the apparent dimensions of the grain boundaries in any given specimen, in part in rather inexplicable ways.

FREEZING STAGE

In this microscope stage the sample is cooled, either with a flow of refrigerated acetone or nitrogen, and the phase changes on cooling and on reheating are watched (Roedder 1962, 1963). Two specific temperatures are normally noted, the eutectic melting temperature (T_e), and the final melting temperature (T_m). The first of these is the temperature during warming at which a completely frozen inclusion, consisting solely of solid salts and ice (and hence nearly opaque), develops enough liquid phase to wet the interfaces between the crystals and become translucent. Although inexact (it can seldom be repeated to better than one or two degrees), it provides a measure of the eutectic melting temperature of the chemical system represented by the inclusion fluid. The final melting temperature (T_m) is the temperature at which the last solid phase (other than the host crystal walls) disappears on warming. This temperature, and the composition of the last phase to melt, when compared with appropriate phase diagrams, place some limits on the composition of the fluid in the inclusion.

HEATING STAGE

Standard petrographic procedures were used, mainly to determine the temperature of disappearance of the vapor bubble (T_h , the temperature of homogenization), but also to determine from their behavior, whether solid crystals within liquid inclusions were daughter crystals, formed on cooling. Under ideal conditions, T_h can be related to the temperature of trapping of an inclusions, but halite is not ideal (see below).

PRESSURE DETERMINATION

Two different methods were used to determine the gas pressure in the inclusions, the crushing stage, and the water dissolution technique. Such data place useful constraints on the origin and geochemistry of the fluids in the inclusions. In the crushing microscope stage the sample is compressed uniaxially, parallel with the microscope optic axis, until a fracture contacts an aqueous inclusion containing vapor bubble (Roedder 1970). The bubble may then collapse or expand. In the water dissolution technique, the sample is immersed in water and watched while a dissolution front approaches the inclusion of interest. In either method, the measurement of the volume of the bubble before and after permits an estimate of the volume expansion. Such a measurement is probably only accurate $\pm 100\%$ at best.

THERMAL GRADIENT MIGRATION

This is test to determine the rate that fluid inclusions migrate in a thermal gradient, such as would be set up around any heat-generating radioactive waste canister. An aqueous liquid inclusion within or between crystals of a soluble salt, when placed in a thermal gradient, will continuously dissolve on the hot side and crystallize on the cold side of the cavity, thus causing the cavity, and its included liquid, to move up the thermal gradient toward the heat source. Inclusion movement is of consequence in the design of a waste

repository, as the included brines are probably more corrosive to possible canister materials than even a saturated NaCl solution.

Several studies (Bradshaw & Sanchez 1969, Holdoway 1974, Jenks 1979) have addressed the problem of the rate of migration of fluid inclusions in salt, experimentally or theoretically. As many variables may affect this rate, and as the interrelations of these variables are not fully understood, experimental determinations are desirable on material from each specific site to be considered.

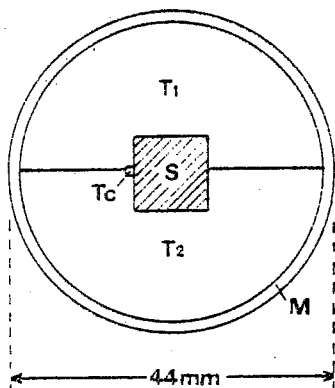


Fig. 1
Cross section of thermal migration experiment sample holder.

The sample (S) consists of a 1×1 cm block of salt, in a closely-fitting slot between two hemicylindrical Teflon blocks (T_1 and T_2), 41 mm in diameter, which fit closely into a closed-end Inconel tube (M) of 1.5 mm wall thickness and 18 cm length. Thermocouples (T_c) are placed along the salt at known positions

In this test, a rectangular block of salt, 1×1 cm in cross section, and containing suitable inclusions, is cut out and the position of the inclusions photographed against a series of fiducial marks. The block is then placed in a 1×1 cm slot in the center of a cylindrical segmented Teflon block (see Text-fig. 1), in tandem with other similar salt blocks, with appropriately placed thermocouple junctions, and the whole assembly is placed in a thermal gradient furnace with appropriate controls for both ambient temperature and superimposed gradient (Roedder & Belkin 1979b). The gradient is established and maintained along the length of the cylinder, perpendicular to the section shown in Text-fig. 1. The cylinder is maintained horizontal. The samples are heated to the desired temperature gradient and ambient temperature slowly ($< 30^\circ\text{C} \cdot \text{hr}^{-1}$) to avoid thermal stress, and then held constant under these conditions for some days. After slow cooling, the samples are rephotographed and movement of the inclusions relative to the fiducial marks is measured.

DATA OBTAINED

WIPP SITE

PETROGRAPHIC STUDIES. Fluid inclusions are a ubiquitous component of the salt crystals making up the host rock at several potential United States nuclear-waste repositories in salt. Results of studies by different investigators of their significance to the possible safety of nuclear-waste repositories ranges from "trivial" to a major concern about repository operations. A continuing study of core from the WIPP site, and comparison with other samples, reveals that much of the apparent discrepancy between various studies (and between various data sets in this study) can be explained by the extreme variability of the amount and nature of the included fluids in the test samples, even in adjacent vertical slabs from the same piece of core. Furthermore, the fluid inclusions commonly show various types of metastability, including both extensive supercooling and stretched liquids under negative pressure (Roedder 1979a, 1971). Additional prob-

lems stem from some seemingly minor details of sample preparation and laboratory technique that may have major effects on the results obtained.

The inclusions consist mainly of two types: (A) original primary; sheets and zones of very minute (mostly $< 5\mu\text{m}$) but dense populations ($\approx 10^{10}\text{ cm}^{-3}$) outlining original cubic hopper growth stages (Pl. 1, Figs 1-2), and (B) recrystallized primary: randomly arrayed, large inclusions (many in range $100\mu\text{m}$ -2mm; Pl. 1, Figs 3-4). About 99% of the total salt examined has recrystallized and forms a matrix for small patches of unrecrystallized hopper salt (Pl. 1, Figs 1-3). Most smaller inclusions are moderately sharp negative cubes; inclusions $> 1\text{ mm}$ become increasingly irregular in shape and size increases. Other inclusions occur along grain boundaries (Pl. 1, Fig. 5). Inclusion water still present in the prepared slabs (by optical measurement of inclusion volumes) ranged from < 0.1 to 1.7 wt.% (avg. 0.36), $> 90\%$ of which was found as $> 1\text{ mm}$ type B inclusions. One set of 3 adjacent parallel vertical slabs from the same piece of core ranged from 0.12 to 0.73 wt.%. Although highly irregular in distribution, the amount of included water is not trivial (see Stewart & al. 1980).

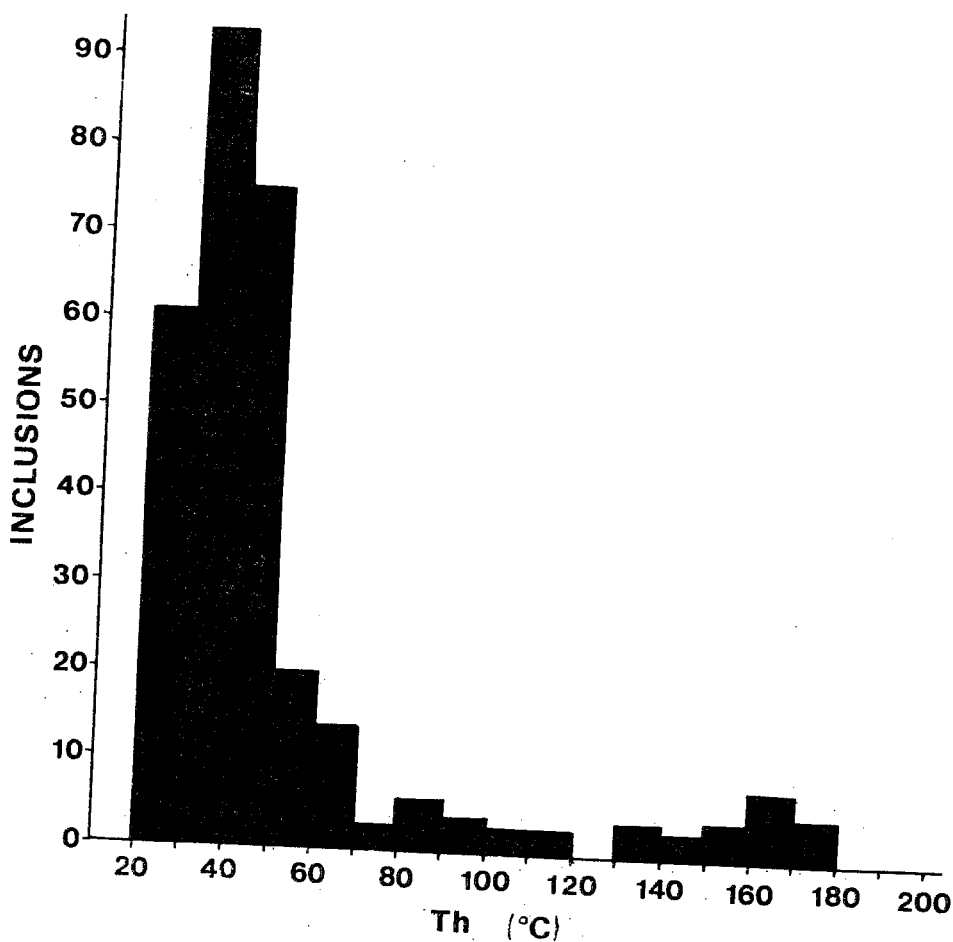


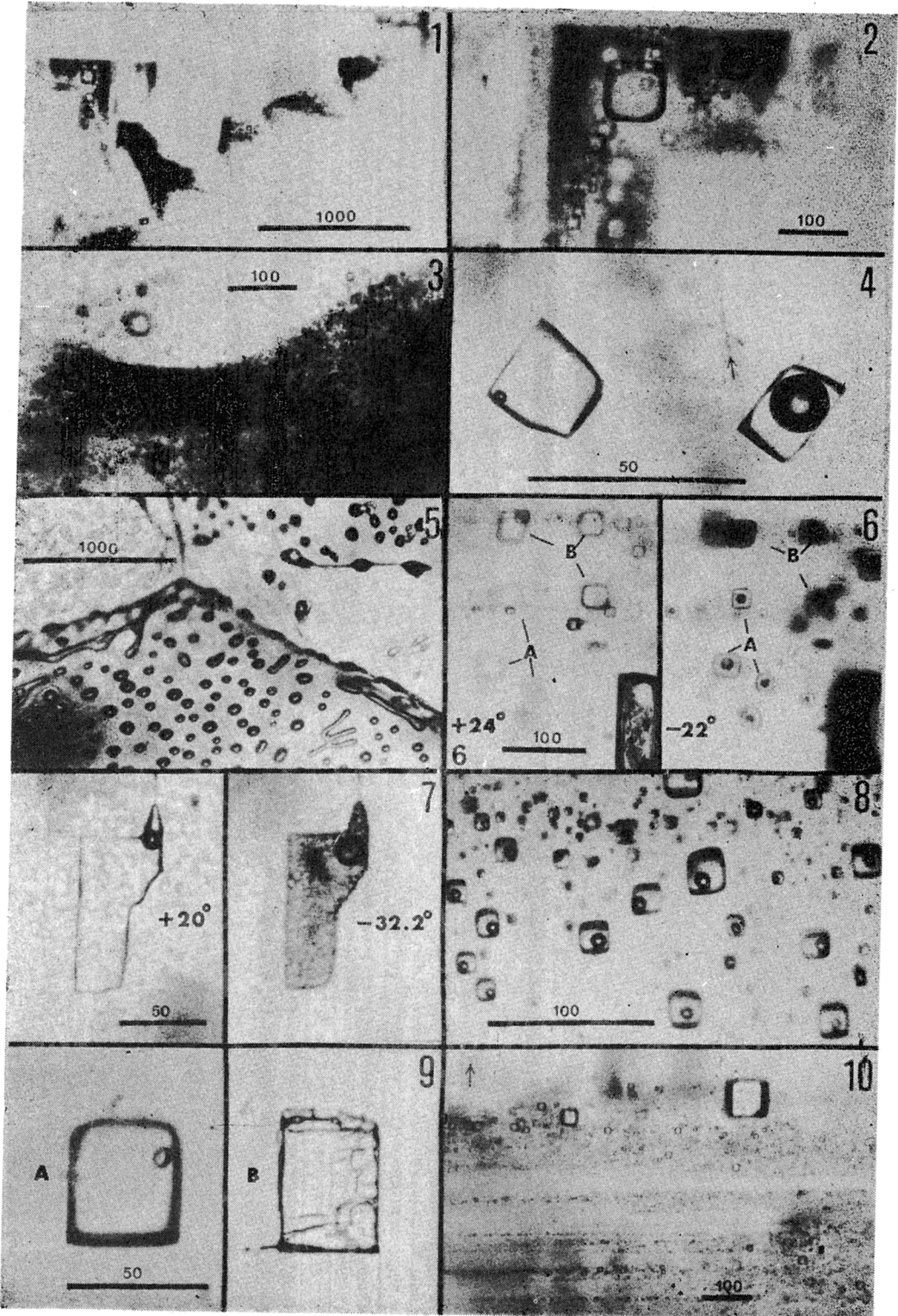
Fig. 2. Homogenization temperatures (T_h) for 317 inclusions from the WIPP site. All values above 80° are believed to be spurious (due to stretching); 11 inclusions homogenizing between 230° and 300° are not plotted

The variability in all measured parameters within a given sample was usually as large as that between samples; very few aspects of the inclusions revealed any consistent relationship to sample depth and hence stratigraphic level. Only one minor example was found in which the fluid composition changed systematically with growth zoning (Pl 1, Fig. 6). The in situ water content, as estimated from coarse intergranular porosity (now open) seen in the cores, must be larger and may well be twice as large as the measured water content.

THERMOMETRIC STUDIES. The larger inclusions ($>100\mu\text{m}$) have a small vapor bubble (≈ 0.1 to 0.3 vol.%) most homogenize at temperatures (T_h) of 20 — 46° (Text-fig. 2). This is the temperature at which expansion of the liquid in these inclusions just eliminates the vapor bubble. Some type B inclusions have one or more different birefringent crystal phases, which I believe, on the basis of highly irregular distribution and heating stage data, to be accidentally trapped solids rather than daughter crystals. These presently unidentified phases include stubby tabular butterfly twin crystals, rounded grains, and length-slow needles that have parallel extinction. Both A and B inclusions show T_e of -23 to

PLATE 1

- 1 — Group of dark, unrecrystallized hopper-salt zones in essentially inclusion-free recrystallized single crystal of halite from sample 2065; See Fig. 2 for detail on group at left
 - 2 — Detail (inverted) of area in Fig. 1, showing sharp crystallographically controlled boundaries probably represent primary crystallization features (i.e., hopper growth) rather than recrystallization
 - 3 — One of the dark areas as in Fig. 1 showing dense cloud of primary type-A inclusions with some primary banding (arrow), and sharp but curving (solution?) contact with crystallographically parallel but almost clear recrystallized salt (at top)
 - 4 — Pair of inclusions in sample 1902. The one on the left is a typical inclusion in recrystallized salt; its small bubble would probably homogenize at $\sim 40^\circ\text{C}$. The one on the right was probably originally similar, but has been reopened via a small crack (arrowed) and the original fluid replaced with a two-phase mixture of gas and liquid. Such large bubbles are usually under high pressure in these samples
 - 5 — Fluid inclusions (gas) on interface between recrystallized salt crystals in sample 2760; Note 120° junction
 - 6 — Two zones of compositionally different inclusions (A and B) in a crystal from sample 2617.2, photographed at the temperatures indicated (focus levels differ slightly). The last crystals to melt in zone A disappeared at -0.1 to 0.0°C , whereas those in B melted between -1.4 and -0.8°C , indicating compositional changes in the fluids during growth. These are primary inclusions as both zones, still with consistent thermal behavior, make a 90° turn
 - 7 — Type-B inclusion in sample 2095.3 taken at the temperatures indicated during a freezing run. At -75.5°C the inclusions contain a partly opaque mixture of solid grains of ice and salts. No change was visible on warming to -34.5°C , but at -32.2°C the mixture suddenly became more translucent and the grain size started to increase, indicating T_e . Extensive melting occurred around -4°C , and the remaining crystals decreased to ~ 20 — 25% at 0°C . These were probably a hydrate but not all $\text{NaCl}\cdot 2\text{H}_2\text{O}$, as a few were present at $+12^\circ\text{C}$, and the last dissolved at $+15^\circ\text{C}$. The room temperature photo was taken after the run. The bubble size varies with phases present and temperature
 - 8 — Group of small primary hopper-growth inclusions in sample 2699.8—2700.0, after 250°C decrepitation run. These inclusions were similar to those in Fig. 2 originally, without bubble, and now each has one as a result of plastic deformation of the host salt. They now homogenize at temperatures as high as 273°C
 - 9 — Inclusion in sample 2760 on crushing stage. "A" shows the inclusion as found. The sample was then stressed and immediately cracked (crack is out of field of view here), but the area of inclusion was still under stress, as changes took place along edges of the inclusion within minutes at constant stress. After 18 minutes (B) the bubble is gone (indicating collapse of the walls) and the changes are pronounced
 - 10 — Unrecrystallized core of grain showing extremely fine banding of primary inclusions with inclusion-free zones between. Top of core is shown by arrow
- All samples (numbers refer to depths in feet) are from core from the ERDA No. 9 borehole, WIPP site, and are viewed in transmitted plain light; Scale bars are in μm



-56°C (Pl. 1, Fig. 7 and Text-fig. 3). The melting of the last solid phase (i.e., T_m , presumably of a hydrate) on warming frozen inclusions occurs at temperatures ranging from to -5 to +15°C. These data require the presence of major amounts of Ca or Mg chlorides; sulfates may also be present. The high concentration of salts (even higher when heated) will greatly reduce the vapor pressure and increase the corrosiveness of the released fluids (see Stewart & al. 1980). Of the many hundreds of inclusions studied, none showed the -21°C T_e characteristic of simple NaCl solutions. Attempts at actual chemical analysis are still in progress. Noncondensable gas content was widely variable, even in seemingly coeval inclusions in the same crystal: some bubbles are essentially a vacuum (i. e., they consist of water vapor only), with $< 10^{-14}$ g (i. e., $< 10^9$ molecules of gases); others (only in B type) contain unidentified gasses under pressures ~ 100 atm at 20°C. In some, this gas was held in solution in the metastable, stretched fluid. The irregular distribution of this gas (Pl. 1, Fig. 4) suggests the presence of a separate immiscible gas phase at some time in the past.

Several types of irreversible and hence irreproducible behaviour were noted on heating. These phenomena were strongly sample dependent, as well as very dependent on both heating rates and temperatures, and hence were not adequately quantified. Most inclusions $> 100\mu\text{m}$, and hence the great bulk of the fluids present, were released by decrepitation at atmospheric pressure in several days at 250°C. Some larger inclusions (~ 1 mm) decrepitated even at 60°C. This decrepitation was in part violent, and caused extensive fracturing and crumbling of the 100-g pieces of core used. Thermal stresses from differential heating were minimized in these runs by keeping heating and cooling rates in the range $0.3\text{--}0.4^\circ\text{C} \cdot \text{min}^{-1}$. The H_2O loss due to decrepitation averaged 0.73 wt.%; in the experiments, the released fluids could only lose enough water to lower their vapor pressures to ~ 1 atm. Less decrepitation and weight loss took place in runs at lower temperatures. Many inclusions $< \sim 100\mu\text{m}$ did not decrepitate, even at 250°C. They became more rounded (in part by dissolution) and expanded $> \sim 5$ vol.% (Pl. 1, Fig. 8) by permanently deforming the host salt, because of the high internal pressure at $> T_h$; the increase in internal pressure with temperature changes abruptly, at T_h from ~ 0.009 to ~ 12 bars $\cdot \text{C}^{-1}$ (Potter 1977). The expansion (and the resulting higher T_h) increased with the maximum temperature attained. Undecrepitated inclusions remaining in decrepitation weight loss runs showed homogenization temperatures of 90–120, 110–180, and 180–273°C, for material from runs at 150, 200 and 250°C, respectively. The expansion is also a function of the original gas pressure in the inclusion and the confining pressure, and pro-

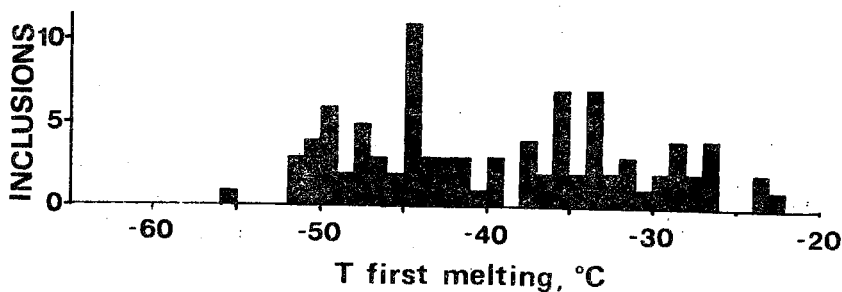


Fig. 3. "Temperature of first melting" (i.e., T_e) for 93 inclusions from the WIPP site

bably of several other variables as well. This "stretching" of the walls can take place even at low temperatures. For example, slowly overheating an inclusion 20°C above its T_h of 20°C caused enough stretching to yield a new T_h of 39°C . Even under isothermal 20°C conditions, visible changes in inclusions volume and shape took place within minutes when the host salt crystal was subjected to uniaxial stress below that necessary to cause a fracture (Pl. 1, Fig. 9).

THERMAL GRADIENT STUDIES. Two quite different processes need to be considered in any study of migration of fluid inclusions in thermal gradients: (1) migration within single crystals, and (2) migration in polycrystalline salt. They will be discussed in that order.

Wilcox (1968) summarized the extensive work (111 references) on the nature and rate of inclusion movement in various substances. Most liquid inclusions move up the thermal gradient, but if the vapor bubble in the liquid is large relative to the liquid, the movement may be in the reverse direction, down the thermal gradient (Wilcox 1969, Anthony & Cline 1972, Chen & Wilcox 1972). The rate of movement is independent of inclusion size in many systems but is strongly (and directly) dependent on inclusion size in others (Wilcox 1968). Even in a given host, many factors may affect the rate of migration, such as gravity, composition and surface tension of the liquid, inclusion size and shape, host-crystal anisotropy, strain and imperfections, external stress, volume percent of vapor bubble and presence of a foreign gas in it. In salt, the rate of movement in a given gradient can be expected to increase as ambient temperature, gradient, and inclusion size increase.

One last caveat on this problem involves the surface tension forces at the bubble/liquid interface. The fluid motions in natural fluid inclusions due to surface tension gradients resulting from thermal gradients are not only extremely fast, but are a function of as-yet unknown compositional variables, and can reverse with changes in the composition or the ambient temperature (Roedder 1962, 1967b).

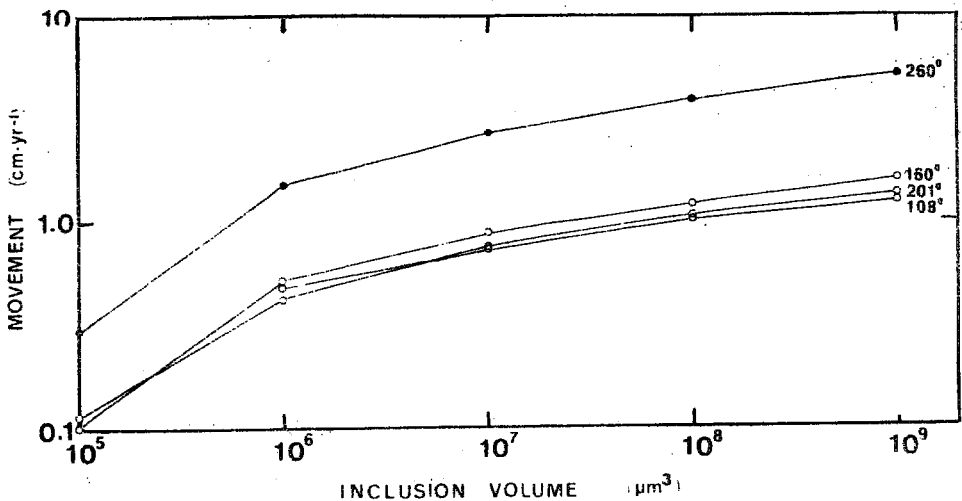


Fig. 4. Migration rates of various sizes of fluid inclusions in salt sample 2061, at $1.5^{\circ}\text{C}\cdot\text{cm}^{-1}$ gradient and the ambient temperatures indicated. Each curve is based on smoothed data for a group (17 to 44) of individual inclusions, run for 72–252 hours. See text for details

In most these experiments, the rectangular sample blocks were cut (very carefully) parallel with the cubic (100) cleavage, but several other orientations were also used. All runs were at $1.5^{\circ}\text{C} \cdot \text{cm}^{-1}$, except as noted. The positions of the inclusions were photographed through the microscope against a series of fiducial marks (both nearby solid inclusions and fine lines scratched on the surface were used). No external stress or pressure was imposed on the sample.

The largest group of data was obtained on sample 2061 and is summarized in Text-fig. 4, the points of which were derived as follows. For a given run, the observed migration rates in $\text{cm} \cdot \text{yr}^{-1}$ for each measured inclusion were plotted (linear scale) against the initial volume of the inclusion in μm^3 (logarithmic scale). A best-fit line was drawn through this data set on the basis of visual estimation. The intersections of this line with inclusion volumes were then plotted log-log as in Text-fig. 4. The original data points from individual inclusions in any given run showed scatter that differed from one sample to another. Many reasons for scatter can be suggested. Most inclusions had no bubble at the start, but all had at temperature used. The inclusions expanded by deformation of the host salt during the slow heat-up period and were presumably liquid-filled during the runs.

Several features of Text-fig. 4 should be noted. First, a rather uniform migration rate takes as inclusion volume decreases. The relatively few inclusions that were flattened perpendicular to, or elongated parallel to direction of motion showed too small deviations in rate for any meaningful quantification of the differences. The rates for the run at 260°C ambient are ~ 3.5 times those found for the other temperature runs for a given volume inclusion. The anomalously low rate for the 201°C run on sample 2061 may be a result of differences within parts of the same samples.

Several runs were made to check the possible effects of the crystallographic orientation of the host relative to the direction of migration. Differences up to a factor of time were found in the rates perpendicular to the dodecahedron (110), the octahedron (111), and the cube (100), but differences of similar magnitude were found for different pieces of the same crystal in the same orientation, and between samples from different core depths. Obviously there must be other, unknown factors involved, either in the crystal or the inclusions.

Small inclusions ($10^4 - 10^5 \mu\text{m}^3$) move so little that many are below the threshold for reliable detection of movement with the method ($\sim 10 \mu\text{m}$). With runs of the durations used here, this threshold corresponded to rates in the range $0.01 - 0.1 \text{ cm} \cdot \text{yr}^{-1}$. Determinations on such small inclusions are of little practical interest, as usually very little of the total water content in any given salt is present as inclusions in this size range (Roedder & Belkin 1979a). Their movement, however, does have some theoretical interest. The best-fit line through the bulk of the data on a plot of movement vs. log initial inclusion volume was generally a straight line that appeared to intersect the ordinate at a threshold volume, below which no movement could be detected, and some inclusions of $\sim 10^5 - 10^6 \mu\text{m}^3$ volume were found not have moved measurably. However, on some of the runs, some inclusions as small as $2 \times 10^4 \mu\text{m}^3$, and hence well below the various apparent intercepts at "zero movement", were found to have migrated small but finite amounts. The sensitivity of the method used was too poor to permit quantification, but these points suggest that perhaps the best-fit line should not intersect the ordinate but should approach it asymptotically.

There is also an indication of a possible thermal gradient threshold for movement, in the distribution of inclusions marking primary hopper growth bands. The banding of inclusion-rich and inclusion-free zones in such hopper

growth bands is very sharp (Pl. 1, Figs 2 and 10). Although not well illustrated by these particular figures, some of the boundaries of inclusion-rich zones have both large and small inclusions aligned along these sharp edges. In view of the observed differential movement of large vs. small inclusions, if there had been even a relatively few μm of movement of these inclusions in the normal geothermal gradient over the 25 million years since these inclusions formed, these sharp boundaries would be blurred. Note, however, that the effect of the small geothermal gradient ($\sim 3 \times 10^{-5} \text{ } ^\circ\text{C} \cdot \text{mm}^{-1}$), driving the inclusions downward, is opposed by the force of gravity, which should drive the inclusions upward (Anthony & Cline 1970).

At the start of this work, some rough scoping experiments at high ambients and/or high gradients were set up to provide guidance for the experimental design of the migration runs. The temperature control and measurement were both much inferior to those used in the runs described above, but the values obtained provide at least some rough indications of the magnitude of the effects. Thus at $\sim 250^\circ\text{C}$ and $4^\circ\text{C} \cdot \text{cm}^{-1}$, an inclusion of $5.5 \times 10^9 \mu\text{m}^3$ moved at $109 \text{ cm} \cdot \text{yr}^{-1}$, and at 320°C and $\sim 20^\circ\text{C} \cdot \text{cm}^{-1}$, inclusions as small as $6.4 \times 10^4 \mu\text{m}^3$ moved at $8.8 \text{ cm} \cdot \text{yr}^{-1}$.

Most inclusions studied in this work were cubic or nearly cubic as found. At the end of the run, after the inclusions had moved tens or hundreds of micrometers, they were still nearly cubic if the original volume was $\leq \sim 2.7 \times 10^9 \mu\text{m}^3$. Larger inclusions were quite different in shape at the end of the run regardless of the ambient temperature used, from 108°C to 260°C . The advancing front surface became smaller though still flat and square in outline, and the sides became curved, forming a tapered, bullet shape. The rear face remained approximately the same size and shape as originally, but a thin sheetlike peripheral fringe of liquid had developed on all four edges, tapering off to the rear (Pl. 2, Fig. 1). It is not known, whether this shape developed early in the run and represents a dynamic equilibrium shape or whether it was still in the process of evolving at the end of the runs. Inclusions forced to migrate perpendicular to (110) and (111) formed similar fringes trailing off the outer edges. Somewhat similar trailing "veils" formed at the edges of migrating flat disk-like inclusions in synthetic KCl (Anthony & Cline 1971).

Since gas-rich inclusions have been found to move down a thermal gradient, a search was made for gas-rich inclusions in the samples that were run in thermal gradients. Only five small gas-rich inclusions were found, with 14–28 vol. % gas. All five were in sample 2061 material and moved down the gradient, toward the cold end, at rates ranging from 0.42 and $0.45 \text{ cm} \cdot \text{yr}^{-1}$ for $9.8 \times 10^8 \mu\text{m}^3$ inclusion at 108°C ambient to $3.10 \text{ cm} \cdot \text{yr}^{-1}$ for $5.5 \times 10^6 \mu\text{m}^3$ inclusions at 160°C ambient. This movement was not only in the reverse direction from that for liquid inclusions, but was 1.25 to 10 times faster than that for liquid inclusions of the same size.

One run yielded a strange result that has yet to be duplicated, but nothing was known to be peculiar in the material used or the operation of the run. The material was sample 2618, cut to yield movement perpendicular to (100). The gradient was 1.5 cm^{-1} and the ambient temperature was 202°C , for 156 hours, a combination that had been used in other runs as well. At the end of the run, however, many of the measured inclusions were found to consist of the separate parts, a small, asymmetric, dumbbell-shaped, vapor-rich inclusion (~ 5 vol. % of original inclusion) that was now on the cold side of the original inclusion location, i.e., it had moved down the gradient, and a larger liquid inclusion, with a vapor bubble, that had moved up the gradient (Pl. 2, Fig. 1). The actual migration

distance of the two individual parts ranged widely from 15 to 725 μm ; all inclusions $> 10^7 \mu\text{m}^3$ in volume (12 total) had liquid moving farther than gas: liquid moved 437 to 725 μm up the gradient, and gas moved 15 to 475 μm down the gradient. Four of the seven inclusions having $< 10^7 \mu\text{m}^3$ volume (down to 1.5×10^5) had gas movements down the gradient that were greater than the corresponding liquid inclusions up the gradient. These movements cannot be converted to rates because the stage during the run when the splitting occurred is unknown; if it occurred at the start of the run, the liquid movements up the gradient yield rates in the same range as that found in other runs that did not exhibit splitting. A very few of the inclusions in some other runs showed similar splitting, but no other run yielded such a consistent splitting, this phenomenon is not understood at present, but there are several possible explanations. The shape of the gas-rich part is also peculiar and Fig. 1 in Pl. 2 shows a typical example at the conclusion of the run; the vapor-rich inclusion consisted of two connected parts, a smaller, flattened, somewhat cubic mass of liquid at the front (in the direction of the movement), and a larger, almost spherical mass of gas (trailing), with a narrower neck between. A similar geometry of liquid and vapor parts of a vapor-rich inclusion moving down gradient has been seen in ADP crystals (Wilcox 1968), but with quite different shapes.

The previous studies have shown that in single salt crystals under the temperatures and gradients expected in nuclear waste repositories, the bulk of the liquid water present as intragranular liquid-filled inclusions would migrate up the gradient at rates in the range of $1 \text{ cm} \cdot \text{yr}^{-1}$. As the average grain size of much rock salt is about 1 centimeter, this movement would result in most inclusions intersecting a grain boundary within a year. In this section, I examine the behavior at this moment of intersection (Roedder & Belkin 1980b).

Parallelepipeds of salt that contained appropriate size fluid inclusions near a grain boundary were cut from core from 2,070.4 to 2,070.6 feet depth at the WIPP site. The grain boundaries (curving) were chosen to have adjacent crystal orientation mismatches of greater than 20° , and were marked by vermiform gas and/or liquid inclusions and dark particles of unidentified impurities that are normal for growth interference boundaries in recrystallized salt. These samples were held in a gradient of $1.5^\circ\text{C} \cdot \text{cm}^{-1}$ at about 150°C ambient for as long as 1,000 hours; they were examined and photographed every 200 to 300 hours.

On intersecting the boundary, the inclusions (originally liquid-filled, with volumes of 10^6 to $10^8 \mu\text{m}^3$) lost 50 to 98 volume percent of their liquid (mainly more than 90 percent). Birefringent daughter minerals precipitated in the remaining liquid, indicating loss of water by evaporation rather than as liquid under these conditions. All resealed themselves to form vapor-rich inclusions and started moving back from the boundary, down the gradient. A few split off a small, even more vapor-rich inclusion that moved down gradient at a higher rate. In contrast with the samples in earlier experiments (Roedder & Belkin 1979a), none of the grain boundaries used here were tight and free of impurities, so none of these inclusions crossed the boundaries. Differences between the experimental conditions and those in an actual repository preclude direct application of the results, but leakage of inclusion fluid along grain boundaries after intersection must be considered as a valid possibility because the stress fields around a canister can hardly be expected to reduce intergranular permeability to zero.

RAYBURN AND VACHERIE DOMES, LOUISIANA

PETROGRAPHY. The results for samples from the two domes, Rayburn and Vacherie were sufficiently similar that the following discussion is generally

applicable to both groups of samples. This lack of differences could be merely a result of the limited number of samples and inclusions tested.

Table 1
Salt samples examined

| Core Box # | Notes | Depth (ft.) |
|----------------------|---|---------------|
| <u>Rayburn Dome</u> | | |
| 4-1 | Dark anhydr.-bearing salt | 168-170 |
| 8-5 | Granular salt | 384-385 |
| 20-15 | Equigranular salt | 1112 |
| | Coarse single crystal salt | 1410 |
| | Coarse single crystal salt | 1450 |
| 32-6 | Coarse single crystal salt ("paleo-spirit level" sample) | 1781.4 |
| 32-7 | Coarse single crystal salt; photographed | 1784.5 |
| 35-14 | Representative coarse single crystal salt | 1971. |
| <u>Vacherie Dome</u> | | |
| 1-6 | Celestite crystals (from cap) | 561 |
| 8-10 | Coarse and fine salt | 885 |
| 11-15 | Coarse single crystal salt | 1067.7 |
| 15-bottom | Granular salt | 1325-1330 |
| 17-18 | Coarse single crystal salt (curved cleavage) with thin boudinaged anhydr. seams | 1432.5 |
| 20-22 | "Megacrystalline salt"; slight odor of H ₂ S on breaking | 1625.5 (base) |
| 27-6 | "Fine-grained", granular salt | 1933-1935 |
| 29-20 | "Megacrystalline" salt | 2083.0 (top) |
| 39-24 | Granular salt | 2655-57 |
| 51-15 | Coarse single-crystal salt adjacent to anhydr. layer; some odor of oil | 3222.5 |

Detailed petrographic descriptions of these cores are being made by others so only those features of particular pertinence to fluid inclusion study will be mentioned here. Table 1 lists the general nature of the samples, and since these samples were taken in part to cover the range of lithologies, they probably are representative of the range. Three types of fluid inclusions were found, brine, compressed gas, and oil; brine was by far the most abundant in volume by

a considerable margin, but compressed gas inclusions were the most numerous. The total volume percent of fluid inclusions evident in these samples is low in all. The distribution is too erratic to permit a good estimate from the available sampling, but it would seem to fall generally somewhere in the range of 0.01 to 0.001 vol. %/o. Only very small portions of the samples examined would approach 0.1 vol. %/o. Some of the large single-crystal samples were essentially free of visible fluid inclusions. All samples contained at least a few anhydrite crystals, and some contained anhydrite-rich bands.

BRINE INCLUSIONS. Some brine inclusions occur as isolated relatively large (≤ 1 mm) inclusions in salt, with or without an included anhydrite crystal (Pl. 2, Figs 2–3). As is generally true in salt, small liquid inclusions without anhydrite are equant negative cubes, and large free inclusions are more irregular (*e.g.*, Pl. 2, Fig. 2). Most brine was found, however, as fillets between adjacent anhydrite crystals, where it is difficult to recognize without strongly convergent illumination (Pl. 2, Figs 4–5). Under normal microscope illumination, such fluid inclusions disappear into the black borders from total reflection at the anhydrite-salt and salt-brine interfaces. This common occurrence of the brine inclusions suggests a preferential wetting, but other brine inclusions, even in anhydrite-rich salt, are not in contact with any anhydrite crystal. Some inclusions appear to be stretched out between two anhydrite crystals; it is possible that such features formed as a result of two adjacent anhydrite crystals, with a fillet of brine between, being pulled apart by flowage of the host salt. As these inclusions are in a large single crystal of salt, presumably there was a subsequent recrystallization. (Some large, clear single crystals of salt now have strongly curved cleavage planes, with a radius of curvature $> \sim 30$ cm).

All but the smallest brine inclusions contain a vapor bubble of ~ 1 vol. %/o (Table 2). Several inclusions were found with dark or opaque specks adhering to the bubble surface; these might well be organic matter (Roedder 1972).

Unfortunately, the origin of most of the inclusions in these samples is obscure at best, as the available criteria (*see* Table III in Roedder 1976) are mostly inappropriate to these samples. Many of the samples contain planes of obvious secondary inclusions parallel to (100) from cleavage, or (110) from shear, that must postdate the host salt. But the large, isolated inclusions within visibly underformed salt, on which most of the work was done, may represent fluids from almost any part of the history of the salt prior to the last recrystallization. Thus they could represent seawater, trapped within the original salt (as in many bedded salts; Roedder & Belkin 1979a), which has coalesced during flowage. They could equally well represent near-surface groundwaters which flowed into fractures in the moving salt dome, and were trapped by rehealing of the host crystal. Inclusions in salt can move and recrystallize so readily (Roedder & Belkin 1980a) that the present shape and occurrence of such inclusions provide no real clues.

COMPRESSED GAS INCLUSIONS. At least a few tiny dark specks (generally ~ 1 – 2 μm) are visible at the contact between most included anhydrite crystals and the host salt (Pl. 2, Figs 4–7) presumably in response to minimum surface energy. These consist of gases under high pressure. Similar high pressure inclusions are found around anhydrite crystals in the “popping salt” of the Winnfield salt dome in Winn Parish, Louisiana (Pl. 3, Fig. 1), and in salt “blowouts” in many other salt domes and anticlines.

OIL INCLUSIONS. Some of the larger inclusions on the surface of anhydrite crystals are strongly colored, generally in browns (Pl. 3, Fig. 2). These are assumed to be oil inclusions, solely on the basis of the color and the odor of petroleum upon breaking some of these samples. Some planes of secondary inclusions

contained three fluids: a host fluid (brine), a tiny bubble of gas with a very much lower index of refraction than the brine, and another bleb of fluid very obviously higher in index than the brine. This last is probably an oil that was present in dispersed droplets in the fluid surrounding this crystal at the time the crack formed. The volume percent of oil varies widely from one inclusion to another.

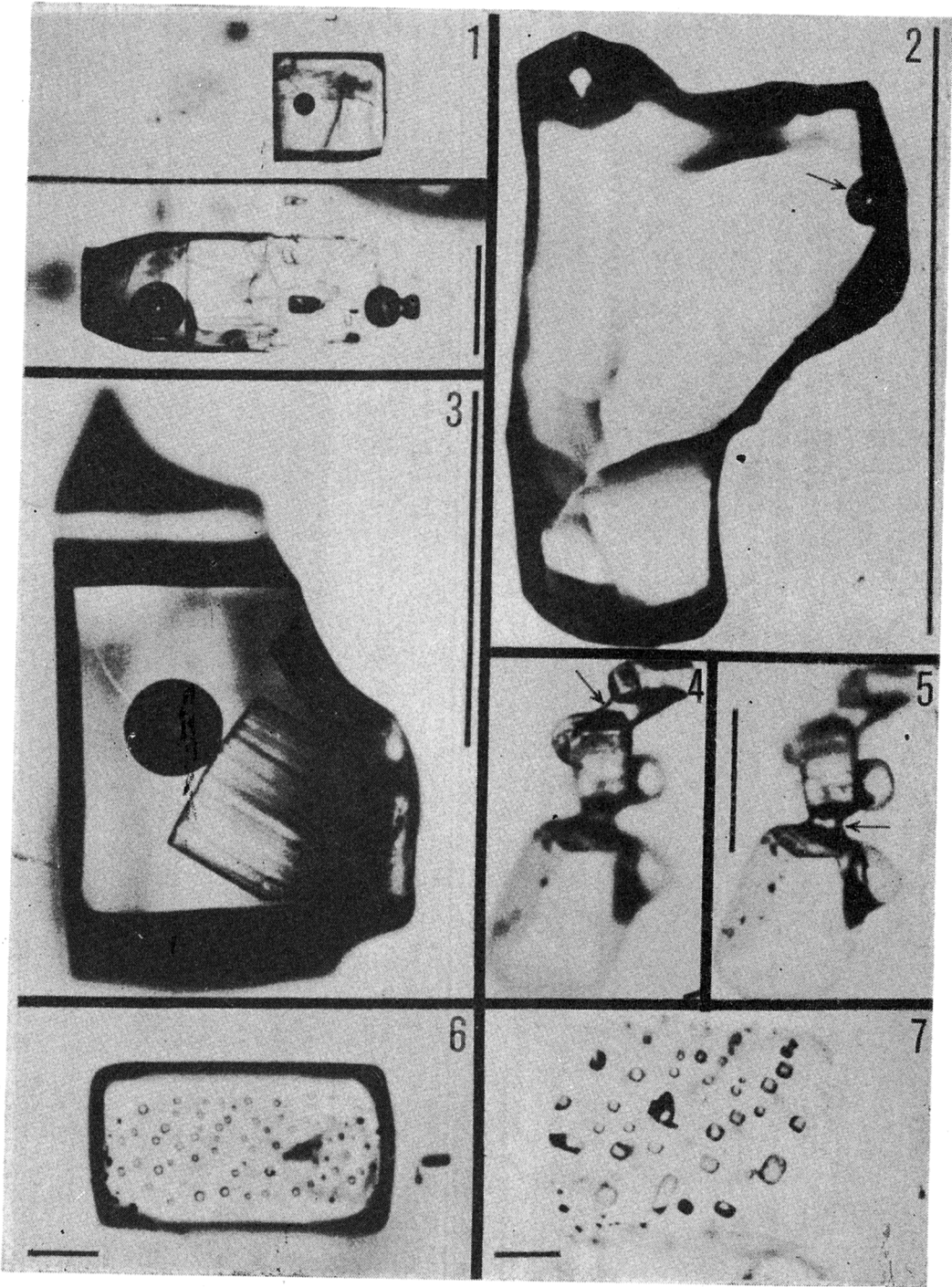
FREEZING STAGE RESULTS. The brine inclusions required temperatures of -67°C to -102°C to freeze; T_e was mostly -21°C to -25°C , and T_m was $\approx +1.0^{\circ}\text{C}$ (see Table 2). The difference between the temperature required for freezing and the final melting temperature T_m represents the amount of supercooling these inclusions underwent before finally nucleating ice and salts. No freezing studies were made of the gas or oil inclusions.

The T_e data given in Table 2 (-21.1°C to -33.1°C , average -23.7°C) are the highest values obtained in several runs on each inclusion. These were chosen because metastable assemblages melt at lower temperatures than the stable ones. Thus in the pure system $\text{NaCl}-\text{H}_2\text{O}$, the stable assemblage at T_e should be hydrohalite ($\text{NaCl}\cdot 2\text{H}_2\text{O}$)-ice-solution at -21.1°C , but as hydrohalite is sluggish to form, the metastable eutectic between NaCl and ice at $\approx -28^{\circ}\text{C}$ (Roedder 1962) is relatively easy to observe. The significance of the T_e values found is that these inclusions must contain fluids that are close to pure $\text{NaCl}-\text{H}_2\text{O}$ mixtures. Only small amounts of other salts are needed to make the change from -21.1°C to the average found here, -23.7°C , or even to the lowest temperature, -33.1°C . In contrast, some inclusions from the WIPP site had T_e as low as -56°C .

The values found for T_m (Table 2) are a further verification of the probability that these inclusions consist of essentially NaCl and H_2O . The fact that these inclusions showed at least some liquid over the range between T_e and T_m is the result of the presence of some small amount of (at present unknown) materials other than NaCl and H_2O . The melting of hydrohalite at temperatures as much as 2.4°C above the known incongruent melting point of the pure compound ($+0.10^{\circ}\text{C}$) is probably a result of the well-known and remarkable sluggishness of

PLATE 2

- 1 — Inclusions in salt sample 2618 before (*above*) and after (*below*) a 156-hour run at 202°C ambient and $1.5^{\circ}\text{C}\cdot\text{cm}^{-1}$ gradient. The large inclusion has split into gas-rich and liquid-rich parts that moved in opposite directions relative to the thermal gradient, which increased to the left. The original position of the inclusion can still be seen, outlined by minute specks of unidentified solids (see *arrows*). The fiduciary mark (a vertical scratch) is visible to the left of the inclusion in the upper photo; it is almost invisible in the lower photo, because of the illumination needed to see the (much larger) bubble, but a series of small specks to the right act as internal reference points; Scale bar= $500\ \mu\text{m}$
- 2 — Large irregular brine inclusion with very small bubble (*arrowed*); Rayburn 1784.5'; Scale bar= $1\ \text{mm}$
- 3 — Large brine inclusion with included anhydrite crystal; Vacherie 1067.7'; Scale bar= $1\ \text{mm}$
- 4 — Group of anhydrite crystals with fillet of adhering brine (*arrowed*) taken in strongly convergent light; Rayburn 1784.5'; Scale bar= $500\ \mu\text{m}$
- 5 — Same group of anhydrite crystals as Fig. 4, at different level of focus, showing another fillet of brine (*arrowed*), in strongly convergent light. In normal collimated microscope lighting, these fillets are hidden in broad black shadows
- 6—7 — Group of semi-oriented inclusions of compressed organic (?) gas at interface between anhydrite crystal and host salt; Rayburn 1784.5'; Scale bars= $100\ \mu\text{m}$



this compound to melt (Adams & Gibson 1930).

HEATING STAGE RESULTS. The homogenization temperatures (*Th*) are low, ranging from 48°C to 111°C, and averaging 72°C (Table 2). The rather large uncertainties in measuring the volume of irregular inclusions causes the lack of correlation with *Th*. Some inclusions have maintained a metastable, "stretched liquid" state, under negative pressure, from failure to nucleate a vapor bubble (Roedder 1967a).

PRESSURE DETERMINATIONS. A total of >100 fluid inclusions and ~30 solid inclusions were tested for gas pressure, mainly by the water dissolution technique. Approximately 95% of those brine inclusions that had an initial bubble

Table 2

Petrographic, heating stage, and freezing stage data on inclusions in halite from salt domes

| Depth /ft/ | Inclusion origin ¹⁾ | Vapor bubble ²⁾ /vol. %/ | Total volume ³⁾ / μm^3 / | Temperature /°C/ ²⁾ | | |
|---------------|--------------------------------|-------------------------------------|--|---------------------------------|---------------------------------|----------------------------------|
| | | | | First melting /T _e / | Final melting /T _m / | Homogenization /T _h / |
| RAYBURN dome | | | | | | |
| 168-170 | P | 0.2 | 1.0x10 ⁵ | -25.4 | +0.3, +0.9, +1.1 | 76,74 |
| " | P | 0.5 | 1.9x10 ⁷ | -- | --- | -- |
| " | S | 1.4 | 1.4x10 ⁵ | -23.2 | +2.4, +2.5 | 85,84 |
| 1410 | P | 3.2 | 1.3x10 ⁷ | -21.1 | +0.2, +0.3 | 100,100 |
| " | P | 1.1 | 9.7x10 ⁶ | -22.5 | +0.6, +0.1 | -- |
| " | P | 1.0 | 4.5x10 ⁷ | -- | -- | >96 ⁴⁾ |
| 1784.5 | P | 1.3 | 1.1x10 ⁵ | -22.5 | 0.0 | 54 |
| " | P | 0.5 | 8.0x10 ⁵ | -24.0 | -1.6, -1.4 | 54 |
| " | P | 0.3 | 1.5x10 ⁵ | -22.0 | 0.0 | 51 |
| " | P | 0.7 | 3.7x10 ⁵ | -23.0 | 0.0, -1.4 | 57.5 |
| " | P | 0.1 | 7.6x10 ⁵ | -23.0 | 0.0, -1.4 | 56 |
| " | P | 0.7 | 5.9x10 ⁵ | -24.0 | 0.0, -1.4 | 54 |
| " | P | 0.7 | 2.1x10 ⁵ | -24.0 | 0.0, -1.5 | 48 |
| " | P | 3.5 | 2.7x10 ⁵ | -24.0 | 0.0, -1.6 | 52 |
| VACHERIE dome | | | | | | |
| 385 | P | 0.5 | 7.8x10 ⁶ | -24.6 | +1.6, +0.9 | 111,110 |
| " | P | 0.2 | 3.9x10 ⁶ | -33.1 | +0.7, +0.5 | 70,71 |
| 1067.7 | P | 0.6 | 4.3x10 ⁶ | -22.5 | +2.1, +1.6 | 109,110 |
| " | S | -- ³⁾ | -- | -22.2 | -1.3, -1.7 | -- |
| 1432.5 | P? | 1.0 | 6.5x10 ⁶ | -25.1 | -1.9, +1.3 | 92,93 |
| " | P? | 2.0 | 3.2x10 ⁶ | -25.2 | +1.9, +1.6, +2.0 | 89,89 |
| 3222.5 | P | 0.5 | 1.4x10 ⁶ | -21.2 | +1.9, +1.3 | 57,58 |
| " | S? | 2.5 | 7.7x10 ⁴ | -21.1 | +2.1, +1.6 | 81,82 |

¹⁾P = primary, S = secondary /both relative to the presently enclosing salt crystal/.

²⁾The results of first and second runs are indicated for some; other, poorer inclusions in some of these samples yielded corroborative data.

³⁾Cannot be determined due to necking down.

⁴⁾Inclusion leaked at 96°C.

⁵⁾Volumes measured at room temperature *after* homogenization runs.

evolved a larger bubble, i.e., they contained gas under > 1 atm (Pl. 3, Figs 3—4). The amount of expansion ranged from 1.4 to ~ 4000 times the original bubble volume, but with no recognizable systematic relation to any observed parameter. As even liquified gases such as CO_2 expand only ~ 350 -fold on converting to a gas, the 4000-fold expansion found for one inclusion from Vacherie that was presumed to be brine can only signify that it originally contained not a water solution, but a volatile liquid, such as liquified hydrocarbon gases under pressure, plus a very small vapor bubble.

The bubble in a few inclusions collapsed completely, indicating the absence of noncondensable gases in these bubbles. This test is exceedingly sensitive, as only 10^9 molecules (i.e., $\sim 10^{-14}$ g) of such gas are needed to make a readily visible bubble several micrometers in diameter (Roedder 1970). When a solid anhydrite crystal was intersected by a fracture or a solution front, a bubble always evolved (Pl. 3, Figs 5—6). Presumably this represents the expansion of the minute gas films and inclusions at the interface between anhydrite and salt. The large expansions observed suggest pressures in the range of hundreds of atmospheres. Inclusions containing mainly CO_2 or CH_4 under high pressure are probably responsible for some of the large spontaneous and disastrous mine "blowouts" of thousands of tons of salt at other salt domes in Louisiana and elsewhere (Pl. 3, Fig. 1; Roedder 1972, p. JJ43).

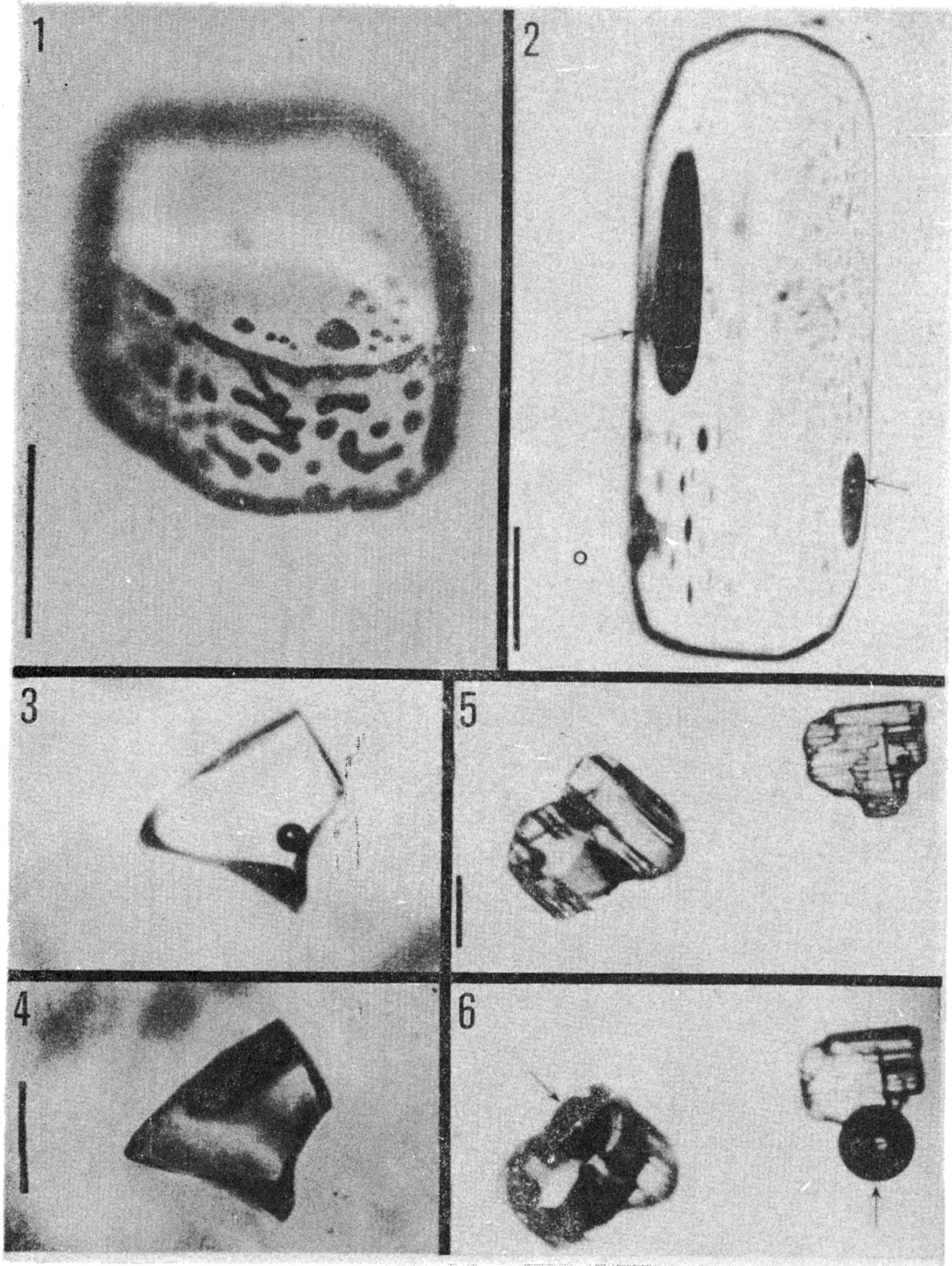
THERMAL MIGRATION RUN. A thermal migration of 180 hours duration was made with a 157°C ambient temperature and a gradient of $1.5^\circ\text{C}\cdot\text{cm}^{-1}$. The rates of migration of 16 inclusions of 10^4 — 10^6 μm^3 volume were in the same range as those obtained for equivalent-sized inclusions in Salado salt from the WIPP salt in the same experiment, i.e., about 0.4 $\text{cm}\cdot\text{yr}^{-1}$ for inclusions of $\sim 10^6$ μm^3 volume, even though the chemical composition is very different. The similarity of these values is of interest, as the lower solubility of NaCl in the strong bitterns present in the Salado salt would be expected to yield significantly lower rates of migration (Roedder & Belkin 1980a).

PALO DURO BASIN, TEXAS

Petrographic examination of several doubly-polished slabs showed that the water in them, in addition to the intergranular water (which continued to creep out slowly over the polished surfaces), is present in three major forms: (1) small to large fluid inclusions in otherwise clear salt; (2) small fluid inclusions attached to or enveloping clusters of crystals of other, birefringent solid phases (or clay

PLATE 3

- 1 — Anhydrite crystal in salt from Winnfield dome, Winn Parish, La, with compressed gas inclusions (*dark*) at interface; Scale bar=100 μm
- 2 — Inclusions of dark brown fluid, presumably oil, with vapor bubbles, (*arrowed*) on surface of anhydrite crystal in salt; Rayburn 1784.5'; Scale bar=100 μm
- 3 — Inclusion with high pressure gas before solution front (above and approximately parallel with plane of photograph) intersects it; Vacherie 1432.5'; Scale bar=100 μm
- 4 — Same field as Pl. 3, Fig. 3 after intersection of solution front with inclusion. All brine has been pushed out and bubble has expanded to fill the inclusion. Total expansion 342-fold
- 5 — Two anhydrite crystals in salt. The solution front is advancing parallel to plane of the photograph but has not yet intersected the inclusions; Scale bar=100 μm
- 6 — Same field as Pl. 3, Fig. 5 after solution front contacts these two crystals; Note large gas bubbles (*arrowed*) formed from almost invisible high pressure gas inclusions



minerals?); so closely spaced that the salt is brownish or even nearly opaque in thicker section; and (3) presumed water in the opaque masses of clay minerals and other as yet unidentified hydrous minerals.

It soon became apparent that estimation of the total water content by optical methods will require independent estimation of the volume fractions of clear salt, brown salt, and opaque masses, plus determinations of their individual water contents. For estimation of the volume fractions, several of the slabs with larger areas of clear salt were checked with a Joyce Loebel Image Analysis System. The entire slab was viewed in uniform transmitted light, and the 64-step gray scale adjusted to span the range from clear salt through brown, slightly clayey salt to opaque masses of clay. A histogram of the frequency of each of the 64 steps (based on averages for points on a 3-mm grid, summed from an original 250,000 sampling points) showed a strongly bimodal distribution. By setting the instrument to discriminate between various ranges of the gray scale, one can get reproducible area percentages for those categories. If the water content of representative parts of each such category can then be determined by independent methods, these values could then be combined with the image analysis system data to obtain total water. As clay masses will be opaque even if less than the full thickness of the plate, this category is best quantized by imaging in reflected light.

A series of freezing runs were made on inclusions in material from sample 696-696.2. Some of these inclusions fractured on freezing, since they had only very small vapor bubbles (many are in the range of only 0.1-0.2 volume % vapor). Inclusions that did not fracture showed T_e generally in the range of -37 to -39°C (inclusions in clear salt) and -51 to -55°C (brown salt).

DISCUSSION OF THE RESULTS

ORIGIN AND HISTORY OF THE SAMPLES

WIPP SITE. These studies have shown no evidence of meteoric water; the primary fluid inclusions trapped in the original salt crystals, as they crystallized in the Permian seas, contained highly saline bitterns that have been largely freed, and in part retrapped, during recrystallization of the bulk of these salt beds at temperatures well under 100°C. This recrystallization of the salt must have taken place at several different times, since the composition of the fluids varies from one inclusion to another. If fresh surface waters had been introduced into these salt beds in the past (as through faulting) and trapped, the resulting inclusions would be simple saturated NaCl solutions and would not have the bittern compositions found. Studies of the stable isotopes of hydrogen and oxygen in the fluid of these inclusions (by J. R. O'Neil; U. S. Geol. Survey, Menlo Park, CA) using rather large (4-23 mg) samples of H₂O that I isolated in the laboratory, also preclude any direct meteoric water source. It is important to note that, at higher temperature, the vapor pressures of bitterns such as are found in the

inclusions would be much lower than those of simple saturated NaCl solutions.

RAYBURN AND VACHERIE DOMES. Of the three types of fluid inclusions that there were found, brine, compressed gas, and oil (in decreasing volume percent abundance), the brine type is most significant. The total amount of such brine is small, certainly < 0.1 vol. % and probably in the range 0.01 to 0.001 volume %, but the inclusions are highly erratic in distribution. Unlike many bedded salt deposits, freezing studies on the brine inclusions in this salt show that they contain fluids that are not far from simple NaCl—H₂O solutions, with very little of other ions such as Ca, Mg and K that are commonly found in large amounts in the inclusions of most bedded salts (Roedder 1963, 1972; Roedder & Belkin 1979a). Fluids containing these other ions, whether they be residual brines from the original evaporation of sea water, or newly-formed brines from diagenetic changes among the several minerals present in the bed, were presumably “kneaded” out of these salt samples during flowage. (Brines high in calcium do occur in some Louisiana dome salts.) The most significant feature, however, is not the lack of such multi-ion fluids, but the fact that there are essentially pure NaCl—H₂O fluids present. Nearly pure NaCl—H₂O fluid in a salt bed can have three possible origins: (1) It can be sea water trapped in the first-formed salt crystals, before evaporation and crystallization caused much buildup of other ions; (2) It can be water evolved by the dehydration of clay minerals or the conversion of other phases such as gypsum to anhydrite during diagenesis; (3) It can be fresh water which has penetrated the salt at some unknown time in the past and been trapped.

The third possibility has the greatest potential importance to the possible use of these domes for nuclear waste storage. At the depth from which these originally bedded salts have flowed to form these domes (≈ 10 —12 km), the fluids in the pores of the surrounding sediments were almost certainly highly saline formation waters, with significant ions other than Na and Cl. But during the rise to the surface, the salt dome must have penetrated aquifers with essentially fresh water. If fracturing occurred during this rise, or subsequently (and the age of these inclusions is unknown), fresh waters could enter the salt and become trapped. The corollary is what if this happened in the past, it might also happen in the future.

The homogenization temperatures found, both for WIPP salt and for these two domes cannot be related to formation temperatures. In addition to the problem of estimating a pressure correction, (were these inclusions formed at the time of the original deep burial (≈ 10 —12 km), during the salt dome ascent, or in essentially the present sample loca-

tions, after dome stabilization?), it is almost certain that some permanent deformation of the inclusion walls from internal pressure can be expected for any inclusions in salt that have been moved from a higher to a lower external pressure. The expansion of fluid inclusions in salt from internal pressure on everheating for days (or even minutes) in the laboratory (Roedder & Belkin 1979a) proves the plasticity of salt under these conditions, and hence the present homogenization temperatures might only represent some rather arbitrary "quench" condition after a long period of sequential "anneals". As an example, one rather large inclusion from Rayburn (volume $2.2 \times 10^7 \mu\text{m}^3$) that originally had a small bubble (0.1%) never did homogenize. The bubble was larger at 230°C than at room temperature, due to this permanent deformation or stretching of the walls. This inclusion also contained gas under pressure.

PALO DURO BASIN. Relatively little has been done with these inclusions but they appear to be rather similar to those from the WIPP site in many aspects. As even similar-sized inclusions in clear and brown salt show major differences in T_e , they must result from real compositional differences and require that different fluids must have been present at different times during the history of these samples. The values in the fifty-below range almost certainly require high concentrations of calcium ion.

WATER CONTENT OF SALT

The *in situ* water content of salt in beds or domes, and the exact nature of its occurrence, are of considerable importance in several aspects of the design and operation of nuclear-waste storage facilities in the salt. Thus, determinations of the water contents of salt samples from various prospective sites are needed early in the site evaluation and selection process. Many such determinations have been made by a wide variety of physical and chemical methods. However, the problems of the determination itself have sometimes been considered trivial or routine. Roedder & Bassett (1981) believe that most determinations of "water" in salt are not truly comparable, that many contain serious and, in part, systematic errors, and that the results are generally on the low side, some by as much as order of magnitude. These problems arise from a combination of the multiple sources of water in the samples, and the sampling, sample preparation, and analytical techniques used. Unfortunately, there is no panacea.

The total water present in a given small sample can be determined by various existing chemical methods. Such determinations may have high precision and may yield accurate results but are subject to two

major short-comings: (1) their validity is seriously limited by the difficulty in obtaining a truly representative sample and by changes in this sample during sample preparation; and (2) even if the sampling and analysis are both correct, an analysis for total water by itself is not very useful. Water is present in rock salt in a variety of forms, and each form may behave differently under the possible conditions of a nuclear-waste storage facility. Hence, each of the major forms present in any given sample must be determined. Most water in rock salt in situ is present in: (1) hydrous minerals (clays, hydrated salts, etc.), (2) intergranular pore fillings, and (3) intragranular fluid inclusions.

The amount of water present in hydrous minerals can be calculated fairly accurately from mineralogical data. The result can sometimes be verified by thermogravimetric analysis or differential thermal analysis on the bulk sample, but water from both opened and unopened fluid inclusions in the sample can make this verification ambiguous.

Intergranular water includes water in "pores" having a wide range of sizes, from microinclusions on grain boundaries to brine pockets having volumes of many cubic meters; its distribution is extremely erratic. Microinclusions on grain boundaries are still present when cores are pulled from the corebarrel, but their rapid loss is plainly indicated by the white efflorescences that commonly form, outlining grain boundaries, on core that has been exposed to air. The resultant water loss is small, however, compared with that from the larger "pores" (≈ 1 cm) that are evident as cavities on some core surfaces. Simple volume estimates indicate that the emptying of a few such "pores" during coring can greatly diminish the amount of intergranular water determined by analysis. Larger brine pockets compound the problem.

In the analysis of water in rock salt, many researchers have used heating times or temperatures that were inadequate for the release of all the water bound in hydrous minerals and, hence, obtained values that were seriously in error on the low side. Even a thorough TGA or DTA study of mixed hydrous phases isolated from rock salt may be difficult to interpret due to the wide temperature ranges over which water may be released from some. Thus, the start of dehydration of gypsum overlaps that of some common smectite clays, and the total range for dehydration of clays includes practically the entire range for that of most other minerals common to salt deposits (some even require temperatures $> 800^\circ\text{C}$). Furthermore, if these minerals are not physically separated from the salt before analysis, water released from fluid inclusions adds to the ambiguity.

If clay or silt is present in the rock salt cores, long heating times may be necessary for dehydration. Thus one 255-g segment of silt-

-bearing rock salt core from the Palo Duro basin, Texas, showed continued weight losses that were almost perfectly linear with time, even after 232 hours in vacuum at 300–352°C (Text-fig. 5). The inset on this figure shows that even small samples of powdered material from this core take over 1 1/2 hours to reach equilibrium weight loss, both at 35°C and at 350°C.

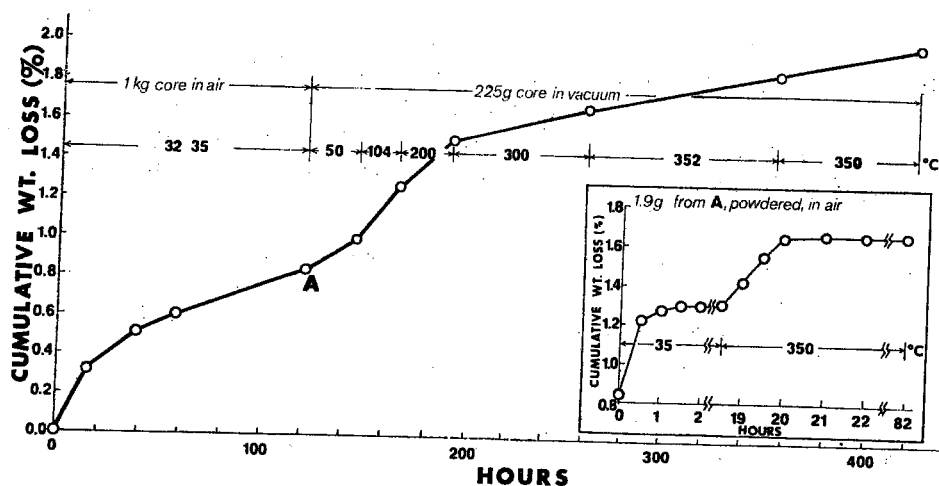


Fig. 5. Weight-loss curve of a silt-bearing rock salt drill core from the Palo Duro Basin, Texas (depth 2604.5–2604.7 ft). The entire piece of core, ≈ 10 cm diameter $\times 10$ cm length, was first dried in air at 32–35°C for 122 hours (to point A). A small part (probably not representative) was powdered and ≈ 2 g heated for 82 additional hours (inset). Another intact 255 h piece of the core from A was then held in vacuum at the temperatures indicated, for an additional 301 hours. The weight loss is believed to be mainly from evolution of water

Intragranular water in fluid inclusions presents a sampling problem that is similar to that for intergranular water, in that a few large inclusions can be equal in volume to millions of small ones. Furthermore, the distribution of such inclusions is extremely erratic, even in adjacent 1-cm-thick slabs cut perpendicular to the bedding. Simple heating has been used to determine intragranular water, and the heating of larger chunks for weight loss (or recovery of evolved water) may help to minimize this sampling problem, but it will generally give low results, for several reasons. For example, some fluid inclusions in salt decrepitate at low temperatures, but if the heating rate is sufficiently low, the inclusions may stay sealed and simply cause the host salt to expand by plastic deformation without release of water, even if the salt contains 1% inclusion water and is heated to 250°C (Pl. 1, Fig. 8). Several other studies report that the salt was ground to a powder before being sampled for water analysis; such grinding will release

most of the inclusion water, and, depending on the relative humidity of the laboratory air at the time, can result in serious water loss or gain.

No amount of analytical precision or accuracy can correct for a non-representative sampling, and increasing sample size is the easiest procedure to minimize this source of trouble. The erratic distribution of water requires that large samples (kilograms, or even tons) be removed from the site, crushed, and quartered down to a representative sample, all without water loss (or gain). The crushing and quartering could be done in a drybox, while gas flows and desiccant monitors indicate total water loss during the process. Aliquots of this sample could then be analyzed by various methods and a correction made for losses in the drybox. Although this procedure would be time consuming and expensive, the importance of valid water determinations may make it worthwhile.

Bedded salts frequently contain over 1% water as liquid inclusions, and may have over 2% total water. Domal salts have one or more orders of magnitude less water than bedded salts, but both are characterized by extreme variation from one point to another.

EXPECTED BEHAVIOR DURING A THERMAL PULSE

The specific behavior of any given type of water during repository operation will certainly vary widely with the many site design and repository parameters. Extrapolation from theoretical or laboratory studies to a real site is difficult indeed. However, certain features of the expected behavior can be outlined, at least qualitatively.

Water in hydrous minerals can be expected to be driven out of the mineral structures near the laboratory-measured dehydration temperatures in air. The actual temperature at which this occurs in the site may be lower, because of the much longer heating times, or higher, from the external confining pressure and the presence of intergranular brines on the grain boundaries.

Intergranular water could flow into the site openings as a result of the hydraulic gradient or lithostatic pressure; salt permeabilities are generally very low, but some of the brine seeps in salt mines might well be a result of just such movement. These fluids may come either from compaction of clay masses, or from squeezing out liquid films between salt crystals. This fluid is also available to flow along any other avenues of pressure release such as fractures that may form during operation of the repository.

Intragranular fluid needs to be distinguished from intergranular fluid because it is not immediately available for such movement in a pressure gradient. However, most fluid inclusions in halite will move

up a thermal gradient (toward the waste canister) at rates that are mainly proportional to the size of the inclusion, the ambient temperature, and the temperature gradient (Roedder & Belkin 1979a). If the grain boundaries are not very clean and tight, a moving liquid inclusion will lose its contents to the grain boundaries (*i.e.*, adding to the intergranular fluid) as soon as it contacts one (Roedder & Belkin 1980b).

The application of the single-crystal migration data to engineering design of a site, e.g. at WIPP, is not simple. The bulk of the water in these beds is probably present in a relatively few large (≥ 1 mm) inclusions whose rates of migration could not be measured by the procedures used. Even in the necessarily biased samples that were used, the bulk of the water was present in the relatively few inclusions ~ 1 mm on an edge. Hence, the maximum migration rates found here (*i.e.*, those for 1 mm³ inclusions) are the most nearly appropriate for calculating a minimum total rate of influx into a canister chamber.

Perhaps the most important aspect of the present work is the discovery that different samples from the same core, and even different parts from the same piece of core, can yield migration rates differing by a factor of 3. As differences of this magnitude exist between the otherwise apparently identical large crystals of salt selected for this study, it would be hazardous to extrapolate these rates to the inclusions in the major part of the salt beds, which consists of smaller crystals than used here. Hence, it would be equally hazardous to extrapolate these rates to a calculation of expected brine inflow in a given storage scenario.

The largest unknown is the behavior of the migrating inclusions when they strike a grain boundary. Depending upon a large number of factors that are mainly unknown at this time, they may be stopped, they may cross the boundary, or they may leak out along the boundary. The route taken by the fluid after an inclusion leaks out into a grain boundary is a complex process that is difficult to quantify with meaningful experiments, due to the uncertain effects of nonuniform thermal and mechanical stress fields on the boundaries.

U. S. Geological Survey,
National Center, Mail Stop 959,
Reston, VA. 22092. USA

REFERENCES

- ADAMS L. H. & GIBSON R. E. 1930. The melting curve of sodium chloride dihydrate. An experimental study of an incongruent melting at pressures up to twelve thousand atmospheres. *Jour. Am. Chem. Soc.*, **52**, 4252-4264.

- ANTHONY T. R. & CLINE H. E. 1970. The kinetics of droplet migration in solids in an accelerational field. *Philosophical Magazine*, 22 (179), 893—901.
- & — 1971. Thermal migration of liquid droplets through solids. *J. Appl. Phys.*, 42, 3380—3387.
- & — 1972. The thermomigration of biphasic vapor-liquid droplets in solids. *Acta Metallurg.*, 20, 247—255.
- BAAR C. A. 1977. Applied salt-rock mechanics, the in-situ behavior of salt rocks. Elsevier; Amsterdam.
- BRADSHAW R. L. & SANCHEZ F. 1969. Migration of brine cavities in rock salt. *J. Geophys. Res.*, 74, 4209—4212.
- CHEN K. H. & WILCOX W. R. 1972. Boiling and convection during movement of solvent inclusions in crystals. *Indus. Eng. Chem. Fund.*, 11, 563—565.
- HOLDWAY K. A. 1974. Petrofabric changes in heated and irradiated salt from Project Salt Vault, Lyons, Kansas. Fourth Sym. on Salt, 1 (A. H. Coogan, Ed.; Northern Ohio Geol. Soc.), 303—312. Cleveland.
- JENKS G. H. 1979. Effects of temperature gradients, stress, and irradiation on migration of brine inclusions in a salt repository. ORNL — 5526, Dist. Cat. UC-70, 67 pp.
- MCCARTHY G. J., ed. 1979. Scientific basis for nuclear waste management, vol. 1, 563 pp. Plenum Press; New York.
- MARTINEZ J. D. & WILCOX R. E. 1976. Hydrologic isolation of mined openings in salt domes, 313—320. In: An investigation of the utility of Gulf Coast salt domes for the storage or disposal of radioactive wastes, OWI-ORNL-Sub-4112-25.
- NORTHRUP C. J. M., Jr., ed. 1980. Scientific basis for nuclear waste management, vol. 2. 936 pp. Plenum Press; New York.
- POTTER R. W. 1977. Pressure corrections for fluid-inclusion homogenization temperatures based on the volumetric properties of the system NaCl—H₂O. *J. Research U. S. Geol. Survey*, 5 (5). 603—607.
- ROEDDER E. 1962. Studies of fluid inclusions I: Low-temperature application of a dual-purpose freezing and heating stage. *Econ. Geology*, 57, 1045—1061.
- 1963. Studies of fluid inclusions II: Freezing data and their interpretation. *Econ. Geology*, 58, 187—211.
- 1965. Mon-Brownian bubble movement in fluid inclusions a thermal gradient detector of extreme sensitivity and rapid response (Abst.). *Geol. Soc. Amer. Special Paper 87, Abstracts for 1965*, 140.
- 1967a. Metastable "superheated" ice in liquid-water inclusions under high negative pressure. *Science*, 155, 1413—1417.
- 1967b. Device for sensing thermal gradients. U. S. Patent No. 3, 344, 699; granted October 3, 1967.
- 1970. Application of an improved crushing microscope stage to studies of the gases in fluid inclusions. *Schweizer. Mineralog. u. Petrog. Mitt.*, 50 (1), 41—58.
- 1971. Metastability in fluid inclusions. *Soc. Mining Geol., Japan. Spec. Issue 3*, 327—334. (Proc. IMA-IAGOD Meetings 70, IAGOD vol.)
- 1972. The composition of fluid inclusions. In: Data of Geochemistry, Sixth Edition, M. Fleischer, Ed., U. S. Geological Survey Professional Paper 440JJ, 164 pp.
- 1967. Fluid-inclusion evidence on the genesis of ores in sedimentary and volcanic rocks. Chapter 4 in: Handbook of strata-bound and stratiform ore deposits, Ed. K. H. Wolf, vol. 2, Geochemical Studies, 67—110. Elsevier; Amsterdam.

- & BASSETT R. L. 1981. Problems in the determination of the water content of rock salt samples and its significance in nuclear waste storage siting. *Geology* (in print).
- & BELKIN H. E. 1979a. Application of studies of fluid inclusions in Permian Salado Salt, New Mexico, to problems of siting the Waste Isolation Pilot Plant, 313—321. In: *Scientific basis for nuclear waste management*, vol. 1, G. J. McCarthy, Ed. Plenum Press; New York.
- & — 1979b. Fluid inclusions in salt from the Rayburn and Vacherie domes, Louisiana. *U. S. Geol. Survey Open File Report 79-1675*, 26 pp.
- & — 1980a. Thermal gradient migration of fluid inclusions in single crystal of salt from the Waste Isolation Pilot Plant site (WIPP), 453—464. In: *Scientific basis for nuclear waste management*, vol. 2, C. J. M. Northrup, Ed. Plenum Press; New York.
- & — 1980b. Migration of fluid inclusions in polycrystalline salt under thermal gradients in the laboratory and Salt Block II (Abst). *Proc. 1980 National Waste Storage Program Information Meeting, ONWI-212*, 361—363.
- STEWART D. B., JONES B. F., ROEDDER E. & POTTER R. W. 1980. Summary of U. S. Geological Survey investigations of fluid-rock-waste reactions in evaporite environments under repository conditions, 335—344. In: *Underground disposal of radioactive wastes*, Atomic Energy Agency; Vienna.
- WILCOX W. R. 1968. Removing inclusions from crystals by gradient techniques. *Indust. Eng. Chem.*, **60**, 13—23.
- 1969. Anomalous gas-liquid inclusion movement. *Indust. Eng. Chem.*, **61**, 76.

E. ROEDDER

ZASTOSOWANIE BADAŃ INKLUZJI DO PROBLEMÓW ZWIĄZANYCH Z PRZECHOWYWANIEM ODPADÓW NUKLEARNYCH W ZŁOŻACH SOLNYCH

(Streszczenie)

Badania inkluzji fluidalnych w próbkach soli (pl. 1—3) z kilku proponowanych miejsc przechowywania odpadów nuklearnych (tab. 1), z zastosowaniem zamrażania, ogrzewania (fig. 1—3 oraz tab. 2) i otwierania inkluzji pod mikroskopem wykazały, że zawartość wysoce aktywnego chemicznie roztworu w inkluzjach zmienia się od $< 0,1$ do $1,7\%$ wag. próbki. Roztwór ten może przemieszczać się w polu termicznym spowodowanym np. przez obecność odpadów nuklearnych z prędkością nawet powyżej 5 cm/rok (fig. 4). Stworzenie użytecznego teoretycznego modelu efektów spowodowanych przez obecność w złożu solnym pojemnika z radioaktywną zawartością wytwarzającą ciepło nie jest obecnie możliwe ze względu na zbyt wiele czynników wpływających w różnym stopniu na prędkość migracji inkluzji roztworu oraz z powodu obecności wody w złożu, także w innych niż inkluzje formach (fig. 5). Natomiast bez takiego wszechstronnie sprawdzonego modelu umieszczanie odpadów radioaktywnych w złożach solnych może spowodować bardzo znaczne skażenie wód podziemnych.